a small difference in the energy of the HOMO as the chalcogen atom is varied from O to S to Se. The LUMO also decreases in energy on going from O to S to Se; however, the energy change is larger. The energy change pattern in the HOMO and LUMO levels for tungsten pyrimidinato complexes is identical with that observed for the $W(dcq)_4(mpic)_{4-n}$ complexes.[33] This, however, is not the case with regard to the two-member molybdenum pyrimidinato series. Here both the HOMO and LUMO increase in energy on going from $Mo(bmpm)_4$ to $Mo(bspm)_4$.

It is also interesting to compare the energy values for $E_{1/2}$ and the MLCT band for the $W(bmpm)_4$ vs the $W(bmp)_4$ complex. For these two complexes, the metal center and the donor atoms remain the same, while the ligand ring structure changes from pyrimidine to pyridine. For these two complexes the energy change in the $E_{1/2}$ values is in the opposite direction as the energy change in the MLCT band. The $E_{1/2}$ values drop from 0.28 to −0.05 V for $W(bmpm)_4$ compared to $W(bmp)_4$; that is, it is easier to oxidize the pyridinato complex. Conversely, a shift to higher energy occurs in the low-energy MLCT band on going from $W(bmpm)_4$ to $W(bmp)_4$. It appears that the effect of replacing the pyrimidine ring with the pyridine ring is to raise the energy of both the HOMO and the LUMO. However, the effect of this change is greater on the LUMO than the HOMO, which is consistent with the assignment of the HOMO as a metal orbital of π-symmetry and the LUMO as a π*-ligand orbital.[33]

Acknowledgment. We thank the Campus Grants Committee of the University of Michigan—Dearborn for financial support.

Contribution from the Department of Chemistry, University of Warwick, Coventry CV4 7AL, U.K., Dipartimento di Chimica, Università di Ferrara, 44100 Ferrara, Italy, and School of Chemistry, University of Bristol, Bristol BS8 1TS, U.K.

Conversion of Hydroxo-Bridged Diplatinum(II) Complexes to Amido-Bridged Diplatinum(II) Complexes. X-ray Crystal Structure of *trans*-$[Pt_2(\mu\text{-}NH_2)_2(Ph_2PO)_2(PPh_2Me)_2]\cdot CH_3CH_2OH$

Nathaniel W. Alcock,[†] Paola Bergamini,*[,‡] Terence J. Kemp,[†] Paul G. Pringle,*[,§] Silvana Sostero,[‡] and Orazio Traverso[‡]

Received March 20, 1990

The amido-bridged diplatinum complexes *cis*- and *trans*-$[Pt_2(\mu\text{-}NH_2)_2(POPh_2)_2(PMePh_2)_2]$ (**1a,b**) as a mixture of isomers has been made by treating $[PtCl_2(dppm\text{-}P,P')]$ with sodium hydroxide in aqueous ammonia or by treatment of $[Pt_2(\mu\text{-}OH)_2(POPh_2)_2(PMePh_2)_2]$ with aqueous ammonia. The mixture **1a,b** has been characterized by ^1H, $^{31}P\{^1H\}$, and $^{15}N\{^1H\}$ NMR spectroscopy, and the X-ray crystal structure of the trans isomer **1a** has been determined (monoclinic, $C2/c$; $a = 25.576$ (10) Å, $b = 14.609$ (4) Å, $c = 26.988$ (10) Å, $\beta = 102.73$ (4)°, $R = 0.045$ for 3478 observed reflections ($I/\sigma(I) \geq 3.0$)). The $[Pt_2N_2]$ ring has a Pt–N bond of 2.114 (7) Å and a dihedral angle of 44 (1)° between the Pt coordination planes. Addition of aqueous ammonia to $[Pt_2(\mu\text{-}OH)_2(PR_3)_4]^{2+}$ complexes gives the corresponding $[Pt_2(\mu\text{-}NH_2)_2(PR_3)_4]^{2+}$ complexes.

Introduction

Until recently, amido complexes of platinum(II) were rare, despite the great interest in ammine–platinum(II) chemistry associated with *cis*-platin. Previous to our report[1] of *trans*- and *cis*-$[Pt_2(\mu\text{-}NH_2)_2(POPh_2)_2(PMePh_2)_2]$ (**1a,b**) the only literature example[2] of a $Pt_2(\mu\text{-}NH_2)_2$ complex was $[Pt_2(\mu\text{-}NH_2)_2(PPh_3)_4]^{2+}$ (**2a**).

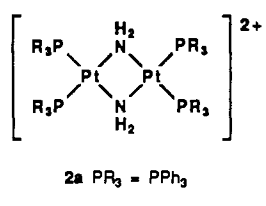

2a $PR_3 = PPh_3$
2b $PR_3 = PPh_2Me$
2c $PR_3 = PPhMe_2$
2d $PR_3 = PMe_3$

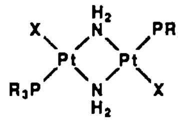

3a X = Me, $PR_3 = PPh_3$
3b X = Me, $PR_3 = PEt_3$
3c X = Me, $PR_3 = PMePh_2$
3d X = H, $PR_3 = PPh_3$
3e X = H, $PR_3 = PEt_3$

More recently,[3,4] the complexes $[Pt_2(\mu\text{-}NH_2)_2(PR_3)_4]^{2+}$ (**2b–d**) and $[Pt_2X_2(\mu\text{-}NH_2)_2(PR_3)_2]$ (**3a–e**) have been characterized. In this paper we describe the details of the synthesis of **1a** and **1b** and the easy conversion of $Pt_2(\mu\text{-}OH)_2$ species into the corresponding $Pt_2(\mu\text{-}NH_2)_2$ species.

Results and Discussion

The chelate $[PtCl_2(dppm\text{-}P,P')]$ (**4**) reacts with NaOH in liquid ammonia or simply with aqueous ammonia to give the *trans*- and *cis*-$[Pt_2(\mu\text{-}NH_2)_2(POPh_2)_2(PMePh_2)_2]$ (**1a,b**) binuclear complexes in high yield (eq 1). The assigned structures for **1a** and **1b** are

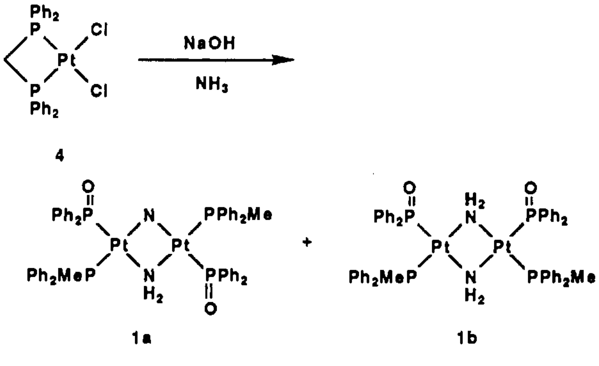

(1)

based on elemental analysis, IR and ^1H, $^{31}P\{^1H\}$, and $^{15}N\{^1H\}$ NMR spectroscopy (see Experimental Section for the data), and an X-ray crystal structure of the trans isomer **1a** (see below).

The $^{31}P\{^1H\}$ and ^1H NMR spectra indicate that the isomers **1a** and **1b** are present in an approximately 1:1 ratio. The ^1H signals for the NH_2 protons occur to high field of TMS and are broad. For the ^{15}N-labeled complexes, these signals are doublets due to ^{15}N–^1H coupling but are still broad. They do not exchange with

---

[†] University of Warwick.
[‡] Università di Ferrara.
[§] University of Bristol.

(1) Alcock, N. W.; Bergamini, P.; Kemp, T. J.; Pringle, P. G. *J. Chem. Soc., Chem. Commun.* **1987**, 235.
(2) Dobinson, A. C.; Mason, R.; Robertson, G. B.; Conti, R. U. F.; Morelli, D.; Cenini, S.; Bonati, F. *J. Chem. Soc., Chem. Commun.* **1967**, 739.
(3) Park, S.; Roundhill, D. M.; Rheingold, A. L. *Inorg. Chem.* **1987**, *26*, 3972.
(4) O'Mahoney, C. A.; Parkin, I. P.; Williams, D. J.; Woollins, J. D. *Polyhedron* **1989**, *8*, 1979.

0020-1669/91/1330-1594$02.50/0

Scheme I. Mechanism A

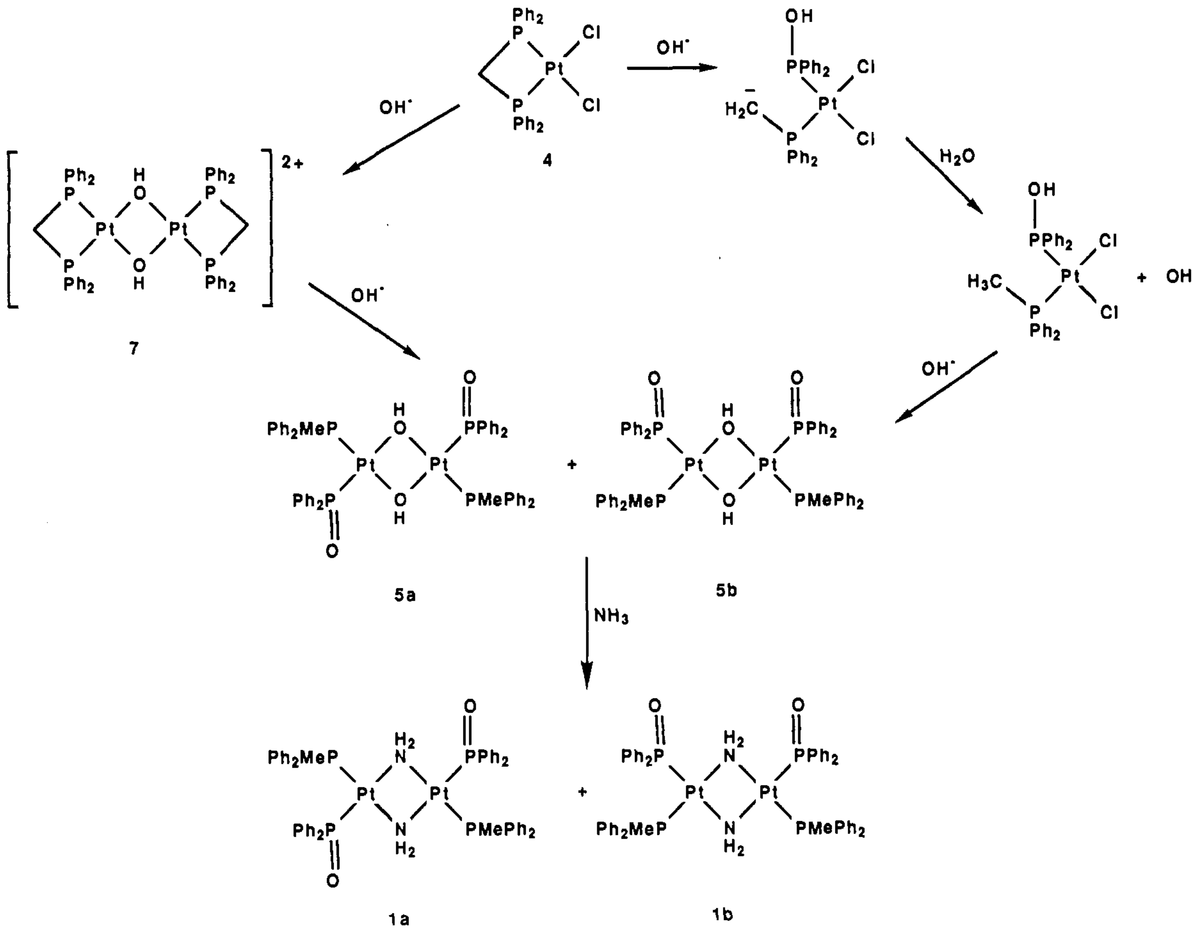

D_2O, and it is therefore concluded that the broadness is due to unresolved ^{31}P or ^{195}Pt coupling. The ^{15}N spectrum shows the three signals expected for **1a** and **1b**, i.e. one signal for **1a** and two signals for **1b**. These are triplets in the approximate ratio of 8:18:8, as would be expected for the central features of the 1:8:18:8:1 multiplet due to coupling to two equivalent ^{195}Pt nuclei.[5]

Crystals of pure *cis*-$[Pt_2(\mu\text{-}NH_2)_2(POPh_2)_2(PMePh_2)_2]$ (**1b**) were grown from $CH_2Cl_2/EtOH$ and when redissolved in $CDCl_3$ showed no indication of isomerization to give the trans isomer **1a** over a period of 20 days. Crystals of pure *trans*-$[Pt_2(\mu\text{-}NH_2)_2(POPh_2)_2(PMePh_2)_2]$ (**1a**) suitable for X-ray crystallography were grown from $CH_2Cl_2/EtOH$. Structurally, *trans*-$[Pt_2(\mu\text{-}NH_2)_2(POPh_2)_2(PMePh_2)_2]$ (**1a**) and *trans*-$[Pt_2Me_2(\mu\text{-}NH_2)_2(PPh_3)_2]$ (**3a**) are similar (Figure 1); both have square-planar-coordinated Pt(II) atoms with dihedral angles between the planes of 44 (1)° in **1a** and 45° in **3a**. The Pt–N distance in **1a** of 2.114 (7) Å is very similar to the 2.13 (1) Å distance reported for **3a**, despite the unsymmetrical substitution of Pt in the latter. The Pt environments in **1a** show one curious feature: despite the chemical equivalence of Pt(1) and Pt(2), the P–Pt–P angles differ by 10°, with a compensating variation in the N_2–Pt–P angles.

Two possible mechanisms for the complex transformation of $[PtCl_2(dppm\text{-}P,P')]$ (**4**) into *trans*- and *cis*-$[Pt_2(\mu\text{-}NH_2)_2(POPh_2)_2(PMePh_2)_2]$ (**1a,b**) are shown in Schemes I and II. Mechanism A involves formation of the binuclear complexes $[Pt_2(\mu\text{-}OH)_2(POPh_2)_2(PMePh_2)_2]$ (**5a,b**) followed by NH_3 addition to exchange the μ-OH for μ-NH_2 ligands with elimination of water. Mechanism B involves formation of the ammine complex $[PtCl(NH_3)(POPh_2)(PMePh_2)]$ (**6**) followed by elimination of HCl. Both mechanisms are plausible and are supported by the following observations on **4** and the isolated intermediates **5a**, **5b**, **6**, and **7**.

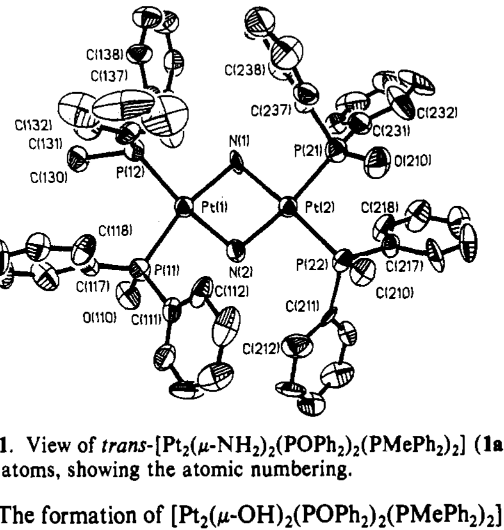

Figure 1. View of *trans*-$[Pt_2(\mu\text{-}NH_2)_2(POPh_2)_2(PMePh_2)_2]$ (**1a**), omitting H atoms, showing the atomic numbering.

(a) The formation of $[Pt_2(\mu\text{-}OH)_2(POPh_2)_2(PMePh_2)_2]$ (**5a,b**) from $[PtCl_2(dppm\text{-}P,P')]$ (**4**) and NaOH in water or DMSO has been reported previously.[6]

(b) Treatment of $[Pt_2(\mu\text{-}OH)_2(POPh_2)_2(PMePh_2)_2]$ (**5a,b**) with aqueous ammonia gives $[Pt_2(\mu\text{-}NH_2)_2(POPh_2)_2(PMePh_2)_2]$ (**1a,b**) quantitatively. Since the complexes $[Pt_2(\mu\text{-}OH)_2(POPh_2)_2(PMePh_2)_2]$ (**5a,b**) are available from $[PtCl_2(PClPh_2)(PMePh_2)]$,[6] this provides an alternative route to $[Pt_2(\mu\text{-}NH_2)_2(POPh_2)_2(PMePh_2)_2]$ (**1a,b**).

(c) The recently reported[7] diplatinum species $[Pt_2(\mu\text{-}OH)_2(dppm\text{-}P,P')_2]^{2+}$ (**7**) reacts rapidly and quantitatively with NaOH

---

(5) Brown, M. P.; Puddephatt, R. J.; Rashidi, M. *Inorg. Chim. Acta* **1976**, *18*, L33.

(6) Bergamini, P.; Kemp, T. J.; Pringle, P. G.; Sostero, S.; Traverso, O. *J. Chem. Soc., Dalton Trans.* **1989**, 2017.

(7) Bandini, A. L.; Banditelli, G.; Cinellu, M. A.; Demartin, F.; Manassero, M.; Minghetti, G. Abstracts, Congresso Interdivizionale della Società Chimica Italiana (CISCI), Perugia, Italy, 1989; p 396.

in water to give $[Pt_2(\mu\text{-}OH)_2(POPh_2)_2(PMePh_2)_2]$ (**5a,b**) or with aqueous ammonia to give $[Pt_2(\mu\text{-}NH_2)_2(POPh_2)_2(PMePh_2)_2]$ (**1a,b**).

(d) We[6] and others[8] have shown that P–C cleavage in complexes of the type $[PtX_2(dppm\text{-}P,P')]$ is a general reaction.

(e) $[PtCl(NH_3)(POPh_2)(PMePh_2)]$ (**6**) is the only product when $[PtCl_2(dppm\text{-}P,P')]$ (**4**) is reacted with liquid ammonia in the absence of NaOH,[9] and treatment of $[PtCl(NH_3)(POPh_2)(PMePh_2)]$ (**6**) with NaOH in ammonia gives $[Pt_2(\mu\text{-}NH_2)_2(POPh_2)_2(PMePh_2)_2]$ (**1a,b**).

The ready exchange of the μ-OH for μ-NH_2 ligands by the action of aqueous NH_3 prompted us to probe the generality of this reaction. $^{31}P\{^1H\}$ NMR experiments reveal that the dicationic hydroxy complexes[10] $[Pt_2(\mu\text{-}OH)_2(PR_3)_4]^{2+}$ (**8a,b**) rapidly react with aqueous ammonia to give the corresponding amido complexes $[Pt_2(\mu\text{-}NH_2)_2(PR_3)_4]^{2+}$ (**2a,b**)[2,4] quantitatively (eq 2). It would therefore appear that $Pt_2(\mu\text{-}OH)_2 \rightarrow Pt_2(\mu\text{-}NH_2)_2$ is a general reaction in phosphine systems whereas the opposite is the norm for ammine systems.[11]

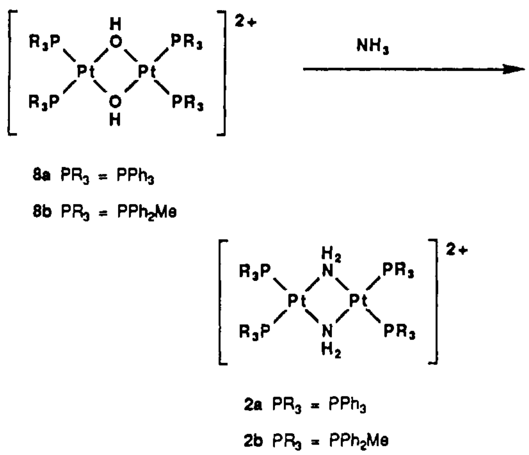

8a $PR_3 = PPh_3$

8b $PR_3 = PPh_2Me$

2a $PR_3 = PPh_3$

2b $PR_3 = PPh_2Me$

(2)

Experimental Section

All NMR spectra were measured at +21 °C by using a Bruker WH 400 spectrometer; chemical shifts are relative to $SiMe_4$ (±0.01 ppm). $^{31}P\{^1H\}$ NMR shifts are to high frequency of 85% H_3PO_4, and $^{15}N\{^1H\}$ NMR shifts are to high frequency of CH_3NO_2. The reactions of $[Pt_2(\mu\text{-}OH)_2(POPh_2)_2(PMePh_2)_2]$ (**5a,b**) and $[Pt_2(\mu\text{-}OH)_2(dppm\text{-}P,P')_2]^{2+}$ (**7**) with aqueous ammonia were carried out by shaking a $CDCl_3$ solution of the complex with aqueous ammonia.

Preparation of *trans*- and *cis*-$[Pt_2(\mu\text{-}NH_2)_2(POPh_2)_2(PMePh_2)_2]$ (1a,b). The complex $[PtCl_2(dppm\text{-}P,P')]$ (0.650 g, 1.0 mmol) was added to a solution of NaOH (2.0 g, 50 mmol) in 30% aqueous ammonia (50 mL) and the resulting suspension stirred vigorously for 16 h. The reaction mixture was then extracted with dichloromethane (3 × 50 mL), the organic phase was separated, dried over sodium sulfate, and filtered, and then the solvent was removed under reduced pressure to yield the white solid product (0.60 g, 98%). The product obtained was pure enough for most purposes but could be recrystallized from CH_2Cl_2/diethyl ether or ethanol. Elemental analysis: C, 49.17 (49.10); H, 4.05 (3.96); N, 2.18 (2.29). IR (Nujol mull): $\nu(NH_2)$ 3360, 3660 (w) cm^{-1}. ^1H NMR ($CDCl_3$), δ: **1a** −0.87 [br, $^1J(^{15}NH) = 69.3$ Hz, NH_2], 1.94 [d, $J(PH) = 8$ Hz, PCH_3]; **1b** −0.34 and −1.62 [br, $^1J(^{15}N) = 68.5, 69.3$ Hz, respectively, NH_2], 2.09 [d, $J(PH) = 10$ Hz, PCH_3]. $^{31}P\{^1H\}$ NMR ($CDCl_3$), δ: **1a** 1.3 [d, $^2J(PP) = 29.7$, $^1J(PtP) = 3308$ Hz], 39.6 [d, $^2J(PP) = 29.7$, $^1J(PtP) = 3230$ Hz]; **1b** 3.1 [d, $^2J(PP) = 19.7$, $^1J(PtP) = 3306$ Hz], 39.8 [d, $^2J(PP) = 19.7$, $^1J(PtP) = 3170$ Hz]. $^{15}N\{^1H\}$ NMR ($CDCl_3$), δ: −408.9 [$J(Pt^{15}N) = 80$ Hz], −412.2 [$^1J(Pt^{15}N) = 84$ Hz], 416.3 [$^1J(Pt^{15}N) = 88$ Hz].

Table I. Atom Coordinates (×10^4) and Temperature Factors (Å^2 × 10^3)

atom	*x*	*y*	*z*	*U*[a]
Pt(1)	3192.1 (2)	8407.1 (4)	5060.8 (2)	36 (1)*
Pt(2)	3453.1 (2)	7550.4 (4)	4097.9 (2)	36 (1)*
P(11)	3464 (2)	7834 (3)	5852 (2)	42 (2)*
P(12)	3100 (2)	9877 (3)	5260 (2)	43 (2)*
P(21)	3668 (2)	8272 (3)	3433 (2)	48 (2)*
P(22)	3897 (2)	6307 (3)	3929 (2)	42 (2)*
O(001)	0	9037 (16)	2500	116 (8)
C(001)	0	8153 (24)	2500	109 (12)
C(002)	460 (14)	7827 (23)	2336 (14)	57 (10)
C(003)	4765 (19)	6960 (32)	2239 (19)	99 (15)
C(004)	4479 (19)	6698 (30)	1821 (19)	91 (14)
N(1)	2963 (5)	8610 (9)	4269 (4)	42 (5)*
N(2)	3209 (6)	7078 (9)	4757 (5)	46 (5)*
O(110)	3070 (5)	7210 (8)	6031 (4)	61 (5)*
O(210)	4182 (5)	7990 (9)	3265 (6)	79 (6)*
C(111)	4092 (6)	7198 (10)	5867 (6)	42 (6)*
C(112)	4451 (6)	7506 (11)	5584 (7)	55 (7)*
C(113)	4934 (7)	7011 (14)	5624 (9)	73 (9)*
C(114)	5019 (8)	6268 (14)	5964 (9)	72 (9)*
C(115)	4670 (8)	6007 (12)	6216 (8)	75 (9)*
C(116)	4200 (7)	6464 (11)	6184 (7)	58 (7)*
C(117)	3733 (7)	8613 (11)	6372 (6)	48 (6)*
C(118)	4183 (7)	9169 (11)	6412 (7)	62 (8)*
C(119)	4354 (8)	9719 (12)	6829 (8)	64 (8)*
C(120)	4119 (9)	9753 (14)	7199 (8)	78 (9)*
C(121)	3691 (8)	9219 (14)	7180 (8)	76 (9)*
C(122)	3478 (8)	8674 (14)	6792 (7)	68 (8)*
C(130)	2783 (6)	10100 (12)	5787 (6)	52 (7)*
C(131)	3699 (7)	10529 (9)	5375 (7)	44 (6)*
C(132)	3874 (8)	11128 (12)	5744 (7)	69 (8)*
C(133)	4326 (8)	11618 (14)	5828 (9)	97 (10)*
C(134)	4675 (9)	11493 (13)	5509 (11)	134 (13)*
C(135)	4521 (9)	10892 (15)	5150 (11)	110 (12)*
C(136)	4052 (7)	10400 (14)	5050 (7)	66 (8)*
C(137)	2651 (6)	10504 (10)	4764 (7)	48 (7)*
C(138)	2731 (7)	11407 (11)	4663 (7)	54 (7)*
C(139)	2364 (8)	11869 (11)	4311 (7)	62 (8)*
C(140)	1906 (8)	11450 (14)	4034 (8)	74 (9)*
C(141)	1810 (7)	10540 (13)	4110 (6)	58 (8)*
C(142)	2199 (7)	10044 (12)	4496 (7)	56 (8)*
C(210)	4605 (6)	6436 (11)	4012 (7)	50 (7)*
C(211)	3835 (7)	5310 (10)	4309 (6)	43 (6)*
C(212)	4096 (8)	5265 (14)	4837 (8)	73 (9)*
C(213)	4090 (8)	4474 (12)	5105 (8)	74 (9)*
C(214)	3821 (7)	3710 (12)	4900 (8)	58 (8)*
C(215)	3529 (8)	3772 (13)	4411 (9)	73 (9)*
C(216)	3549 (7)	4532 (11)	4112 (6)	51 (7)*
C(217)	3639 (6)	5910 (10)	3285 (6)	42 (6)*
C(218)	3115 (7)	5941 (11)	3091 (7)	59 (8)*
C(219)	2891 (8)	5650 (12)	2590 (7)	74 (9)*
C(220)	3244 (9)	5314 (14)	2312 (9)	85 (10)*
C(221)	3765 (8)	5245 (14)	2517 (8)	77 (9)*
C(222)	3967 (8)	5512 (14)	2995 (6)	71 (8)*
C(231)	3128 (8)	8217 (10)	2878 (7)	56 (7)*
C(232)	3233 (11)	8267 (14)	2404 (8)	95 (11)*
C(233)	2818 (14)	8254 (14)	1980 (7)	117 (14)*
C(234)	2265 (13)	8186 (16)	2035 (10)	106 (13)*
C(235)	2147 (11)	8105 (13)	2496 (10)	93 (11)*
C(236)	2587 (7)	8124 (10)	2930 (6)	56 (7)*
C(237)	3734 (6)	9504 (10)	3537 (6)	43 (6)*
C(238)	3282 (7)	10110 (11)	3486 (6)	51 (7)*
C(239)	3356 (8)	11030 (11)	3562 (7)	63 (8)*
C(240)	3855 (8)	11370 (13)	3684 (8)	77 (9)*
C(241)	4310 (8)	10805 (13)	3719 (9)	80 (10)*
C(242)	4218 (7)	9885 (11)	3673 (6)	47 (7)*

[a] Starred values denote equivalent isotropic *U* defined as one-third of the trace of the orthogonalized U(*ij*) tensor.

Preparation of $[PtCl(NH_3)(POPh_2)(PMePh_2)]\cdot H_2O$ (6). A solution of $[PtCl_2(dppm\text{-}P,P')]$ (0.50 g, 0.77 mmol) in liquid ammonia (300 mL) was stirred at −50 °C for 10 min. The temperature was then allowed to

---

(8) Lin, I. J. B.; Lai, J. S.; Liu, C. W. *Organometallics* **1990**, *9*, 530.

(9) The source of the oxygen in the reaction to give $[PtCl(NH_3)(POPh_2)(PMePh_2)]$ (**6**) is adventitious H_2O in the liquid ammonia, which was deliberately not dried; when NH_3 distilled from sodium was used, a complex mixture of unidentified products was formed. The geometry of $[PtCl(NH_3)(POPh_2)(PMePh_2)]$ (**6**) is consistent with the spectroscopic data, but it is possible that the relative positions of the Cl and NH_3 are reversed.

(10) Bushnell, C. W.; Dixon, K. R.; Hunter, R. G.; McFarland, J. J. *Can. J. Chem.* **1972**, *50*, 3694.

(11) For example, see: Faggiani, R.; Lippert, B.; Lock, C. J. L.; Rosenberg, B. *J. Am. Chem. Soc.* **1977**, *99*, 777.

Scheme II. Mechanism B

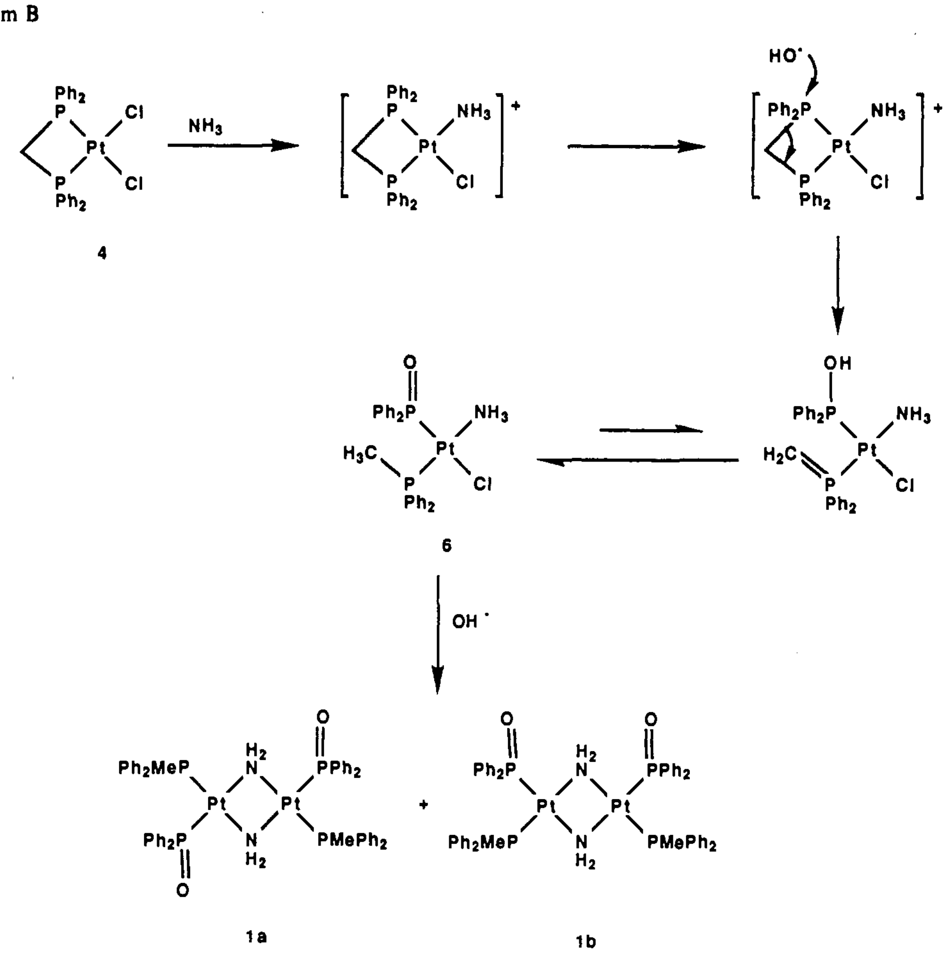

rise and the ammonia to boil off. After 3 h the solvent had evaporated to leave a pale yellow solid, which was then treated with water (50 mL) and CH_2Cl_2 (2 × 50 mL). The organic layer was then separated, dried over Na_2SO_4, and filtered and finally the solvent evaporated at reduced pressure to give the product, which was washed with small portions of acetone (5 × 5 mL). The yield was 0.25 g (49%). Elemental analysis: C, 45.08 (45.05); H, 3.89 (4.23); N, 2.08 (2.10); Cl, 5.48 (5.32); P, 9.42 (9.3); MW 656 (666.5). IR (CsI disk): $\nu(NH_3)$ 3330, 3300 (m) cm^{-1}; ν(PtCl) 275 cm^{-1}. ^1H NMR ($CDCl_3$), δ: 2.75 [br t, $^2J(PtH) = 41$ Hz, NH_3], 1.9 [d, $^2J(PH) = 11.2$, $^3J(PtH) = 45$ Hz]. $^{31}P\{^1H\}$ NMR ($CDCl_3$), δ: −3.5 [d, $^2J(PP) = 23$, $^1J(PtP) = 3915$ Hz], +34.7 [d, $^2J(PP) = 23$, $^1J(PtP) = 3561$ Hz)].

Crystal Structure of 1a. Crystal Data for $C_{50}H_{48}N_2O_2P_4Pt_2 \cdot C_2H_5OH$: monoclinic, space group $C2/c$, $a = 25.576$ (10) Å, $b = 14.609$ (4) Å, $c = 26.988$ (10) Å, $\beta = 102.73$ (4)°, $V = 9835$ (8) $Å^3$, MW = 1269.2, $Z = 8$, $D_c = 1.72$ g cm^{-3}, Mo Kα radiation, $\lambda = 0.71069$ Å, μ(Mo Kα) = 58.8 cm^{-1}, $F(000) = 4752$. Crystal character: colorless laths. Data were collected with a Syntex $P2_1$ four-circle diffractometer. Maximum 2θ was 40° (the crystal scattering very weakly at higher angles), with scan range ±0.85 (2θ) around the Kα_1–Kα_2 angles and scan speed 3–29° min^{-1}, depending on the intensity of a 2-s prescan; backgrounds were measured at each end of the scan for 0.25 of the scan time. Three standard reflections were monitored every 200 reflections and showed slight changes during data collection; the data were rescaled to correct for this. Unit cell dimensions and standard deviations were obtained by least-squares fit to 15 high-angle reflections. A total of 3478 observed reflections ($I/\sigma(I) > 3.0$) were used in refinement (12174 reflections examined; 6076 unique; $R_{merge} = 0.022$) and corrected for Lorentz, polarization, and absorption effects (by Gaussian integration); maximum and minimum transmission factors were 0.64 and 0.42. The crystal dimensions were 0.26 × 0.39 × 0.17 mm. Systematic absences: hkl, $h + k \neq 2n$; $h0l$, $l \neq 2n$. The heavy atoms were located by Patterson techniques, and the light atoms were then found on successive Fourier syntheses. Identification of the amide nitrogen atoms and the methyl and oxo groups on the phosphorus atoms was based partly on their satisfactory behavior during refinement and partly on the chemical evidence. Hydrogen atoms were given fixed isotropic temperature factors, $U = 0.07$ $Å^2$. Those defined by the molecular geometry were inserted at calculated positions and not refined; methyl and amide hydrogen atoms were omitted. Two disordered solvent molecules were identified, located near 2-fold axes, presumed to be EtOH. They were modeled by one oxygen and one carbon, on a 2-fold axis, and four carbon atoms in general positions, at 0.5 occupancy. Because of this disorder, it is not clear exactly what proportion of solvent is present, but it is assumed to represent about one molecule per Pt_2 unit. As it is distant from the Pt complex, this solvent is not expected to have any appreciable influence on the refined coordinates for the complex. Final refinement was by cascaded least-squares methods, with anisotropic temperature factors for all atoms other than hydrogen and solvent atoms, refining 557 parameters. The largest peaks on a final difference Fourier synthesis were of height 2.0 e $Å^{-3}$ (near the Pt atoms). Apart from these ripples, the largest peaks (approximately 1.1 e $Å^{-3}$) were in positions appropriate to amido H atoms, but they were insufficiently defined to be included with confidence. A weighting scheme of the form $w = 1/(\sigma^2(F) + gF^2)$ with $g = 0.007$ was used. This was shown to be satisfactory by a weight analysis. The final R value was 0.045 ($R_w = 0.048$). Computing was with the SHELXTL system[12] on a Data General DG30 computer. Scat-

Table II. Selected Bond Lengths and Angles

	Bond Lengths (Å)		
Pt(1)–P(12)	2.239	Pt(1)–P(11)	2.256 (4)
Pt(1)–N(2)	2.112 (13)	Pt(1)–N(1)	2.109 (11)
Pt(2)–P(22)	2.241 (4)	Pt(2)–P(21)	2.252 (5)
Pt(2)–N(2)	2.127 (14)	Pt(2)–N(1)	2.107 (13)
P(11)–C(111)	1.846 (17)	P(11)–O(110)	1.515 (13)
P(12)–C(130)	1.814 (20)	P(11)–C(117)	1.821 (16)
P(12)–C(137)	1.809 (16)	P(12)–C(131)	1.772 (16)
P(21)–C(231)	1.806 (18)	P(21)–O(210)	1.537 (15)
P(22)–C(210)	1.783 (17)	P(21)–C(237)	1.824 (16)
P(22)–C(217)	1.811 (16)	P(22)–C(211)	1.808 (16)
	Bond Angles (deg)		
Pt(1)–N(1)–Pt(2)	94.1 (5)	N(2)–Pt(1)–P(11)	89.8 (4)
Pt(1)–N(2)–Pt(2)	93.5 (5)	N(2)–Pt(2)–P(22)	99.3 (4)
N(1)–Pt(1)–P(12)	95.0 (4)	P(11)–Pt(1)–P(12)	99.0 (2)
N(1)–Pt(2)–P(21)	95.3 (4)	P(21)–Pt(1)–P(22)	89.6 (2)

---

[12] Sheldrick, G. M. *SHELXTL Users Manual*; Nicolet XRD Corp.: Madison, WI, 1983.

tering factors in the analytical form and anomalous dispersion factors were taken from ref 13. Final atomic coordinates are given in Table I, and selected bond lengths and angles in Table II.

Acknowledgment. We thank NATO for the provision of a travel grant, the British Council (Rome) for support, and Johnson-Matthey plc for a generous loan of platinum salts.

Supplementary Material Available: Tables of full bond lengths and angles, anisotropic thermal parameters, and H atom coordinates (4 pages); a listing of structure factors (21 pages). Ordering information is given on any current masthead page.

---

(13) *International Tables for X-ray Crystallography*; Kynoch Press: Birmingham, U.K., 1974; Vol. IV.

Contribution from the Departments of Chemistry, University of South Carolina,
Columbia, South Carolina 29208, and Furman University, Greenville, South Carolina 29613

Calculations for Various Structural Forms of $B_{12}H_{12}^{2-}$ as Clues to the Possible Mechanisms for the Isomerizations of $C_2B_{10}H_{12}$

Benjamin M. Gimarc,[*,†] D. Scott Warren,[†] Jane J. Ott,[‡] and Carl Brown[‡]

Received August 10, 1989

We report the results of geometry-optimized AM1 and ab initio SCF-MO calculations at the STO-3G level for $B_{12}H_{12}^{2-}$ in several structural forms that represent intermediates in various mechanisms proposed for the isomerization of the carboranes *o*-, *m*-, and *p*-$C_2B_{10}H_{12}$. We assume that the energies of the $B_{12}H_{12}^{2-}$ structures, relative to that of the regular icosahedron, represent estimates of activation barriers that the corresponding carboranes might meet along the proposed mechanisms. Structures studied were the regular icosahedron (I_h), an icosahedron of D_{3h} symmetry, the cuboctahedron (O_h), the bicapped pentagonal prism (D_{5h}), the anticuboctahedron (D_{3h}), the tetracapped cube (D_{4h}), the truncated tetrahedron (T_d), and a hexagonal antiprism (D_{6d}). Structural parameters and total energies of these structures are tabulated. Each mechanism can be represented by a reaction graph, the connectivity of which describes the pattern of isomeric conversions for $C_2B_{10}H_{12}$. An acceptable mechanism must have a low activation barrier and require minimal atomic motions, and its reaction graph must account for the experimental observations of isomerizations. The lowest energy pathway seems to be one involving triangular-face rotation. Next higher in energy is the mechanism that passes through the cuboctahedral structure. Carborane isomerization reactions pass through specific transition-state isomers. Lacking calculated energies for these isomers, one can estimate their relative stabilities qualitatively by empirical valence rules and the rule of topological charge stabilization. These considerations give insight into the details of individual processes and, together with the calculated energy results for $B_{12}H_{12}^{2-}$, provide new support for triangular-face rotation as the mechanism that can best account for the observed isomerizations of *o*-, *m*-, and *p*-$C_2B_{10}H_{12}$.

Introduction

The polyhedral carboranes, $C_2B_{n-2}H_n$, are related to the *closo*-boranes, $B_nH_n^{2-}$ ($5 \leq n \leq 12$). The boron or carbon atoms are linked together to form polyhedral structures with triangular faces. A hydrogen substituent is attached in the position exo to each boron or carbon. The carboranes share the structures of corresponding borane dianions; in each case, two carbon atoms replace a pair of B^- entities. The location of the carbon heteroatoms in the polyhedral cage creates the possibility of positional isomers, and indeed two or more isomers are known for the carboranes where $n = 5, 6, 7, 10$, and 12. For icosahedral $C_2B_{10}H_{12}$, three isomers are possible (**1**–**3**) and all three have been prepared and characterized.[1–3] The two carbons can be separated by paths of a single-bond distance (1,2, **1**), two bond lengths (1,7, **2**), or three bond lengths (1,12, **3**). Occasionally, the three isomers are referred to as ortho, meta, or para, respectively. Relative stabilities of the three isomers have been rationalized by empirical valence rules[4,5] and the rule of topological charge stabilization,[6] substantiated by the results of ab initio SCF–MO calculations,[7] and confirmed by experimental observations of thermally induced interconversions among the isomers. These methods all agree that the para isomer (1,12) is more stable than the meta (1,7), which in turn is more stable than the ortho isomer (1,2). Heating at 500 °C converts 1,2 into 1,7. At higher temperatures (615 °C), only small amounts of the 1,12-isomer are formed as 1,7-$C_2B_{10}H_{12}$ decomposes.[3] Experiments with substituted 12-atom *closo*-carboranes and -boranes tend to confirm the conclusion that 1,2- and 1,7-isomers interconvert but do not easily rearrange to the 1,12-isomer and that isomerizations occur intramolecularly.[8] The activation barrier to rearrangement of 1,2-$C_2B_{10}H_{12}$ is 62 kcal/mol.[9] The barrier to $B_{12}H_{12}^{2-}$ rearrangement has been estimated to exceed 80 kcal/mol.[10]

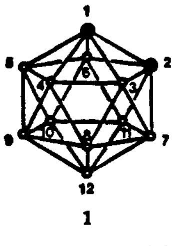

1

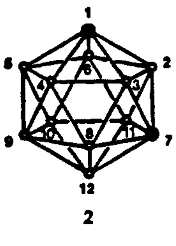

2

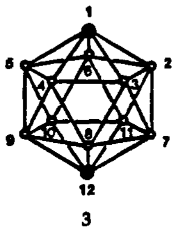

3

Intramolecular thermal isomerizations have been observed to occur in other carboranes as well. In these framework reorganizations, bonds break and are replaced by new bonds and carbon heteroatoms are shifted to new positions, but the process occurs in such a way that the original structural form of the polyhedron is restored. Twenty-five years ago, Lipscomb proposed a general mechanism for the isomerization of the *closo*-boranes and -carboranes. In a classic review,[11] Lipscomb suggested that the re-

---

[†] University of South Carolina.

[‡] Furman University.

(1) Potenza, J. A.; Lipscomb, W. N. *Inorg. Chem.* **1966**, *5*, 1471–1477, 1478–1482, 1483–1488.

(2) Potenza, J. A.; Lipscomb, W. N. *Proc. Natl. Acad. Sci. U.S.A.* **1966**, *56*, 1917–1919. Beall, H.; Lipscomb, W. N. *Inorg. Chem.* **1967**, *6*, 874–879.

(3) Papetti, S.; Heyling, T. L. *J. Am. Chem. Soc.* **1964**, *86*, 2295.

(4) Williams, R. E.; Gerhart, F. J. *J. Am. Chem. Soc.* **1965**, *87*, 3513–3515.

(5) Williams, R. E. In *Progress in Boron Chemistry*; Brotherton, R. J., Steinberg, H., Eds. Pergamon: Oxford, England, 1970; Vol. 2, p 37.

(6) Ott, J. J.; Gimarc, B. M. *J. Am. Chem. Soc.* **1986**, *108*, 4303–4308.

(7) Ott, J. J.; Gimarc, B. M. *J. Comput. Chem.* **1986**, *7*, 673–692.

(8) Hertler, W. R.; Knoth, W. H.; Muetterties, E. L. *J. Am. Chem. Soc.* **1964**, *86*, 5434–5439.

(9) Salinger, R. M.; Frye, C. L. *Inorg. Chem.* **1965**, *4*, 1815–1816.

(10) Muetterties, E. L.; Knoth, W. H. *Polyhedral Boranes*; Marcel Dekker: New York, 1968; p 69.

0020-1669/91/1330-1598$02.50/0